Original Research Article

Innovative Approaches to Bengal gram Yield Mapping: Integration of Sentinel-1 SAR and Crop Simulation Models for Precision Agriculture

ABSTRACT

Accurate spatial yield estimation is crucial for optimizing agricultural management and ensuring food security. This study integrates Sentinel-1A SAR remote sensing data and the DSSAT crop simulation model to predict Bengal gram (chickpea) yield in Nagaur district, Rajasthan, India. Sentinel-1A backscatter data were processed for crop area mapping, achieving an overall classification accuracy of 85.1% and a kappa index of 0.70, demonstrating the reliability of SAR for agricultural monitoring under diverse weather conditions. Leaf Area Index (LAI) was derived from SAR backscatter values and linked to DSSAT-simulated yields, generating spatial yield predictions. Validation using Crop Cutting Experiment (CCE) data showed a high agreement of 91.3% between predicted and observed yields, with low root mean square error (RMSE), confirming model accuracy. This research highlights the synergistic potential of SAR-based remote sensing and simulation models for large-scale yield forecasting, advancing precision agriculture. Future efforts may incorporate additional sensors and machine learning to further enhance prediction accuracy and adaptability to climate variability.

Keywords: Backscatter value, crop simulation model, remote sensing, SAR data

1. INTRODUCTION

Agricultural productivity plays a vital role in ensuring global food security. Estimating crop yield accurately across diverse spatial and temporal scales is essential for effective agricultural planning and management. Traditional yield estimation techniques rely heavily on ground-based surveys, which, although accurate, are time-consuming, labor-intensive, and limited in spatial coverage. In recent years, advancements in remote sensing technologies and crop simulation models have transformed agricultural yield estimation by providing scalable, timely, and cost-effective solutions.

Remote sensing offers a wealth of geospatial data from various satellite platforms, enabling continuous monitoring of crop growth conditions. Sentinel-2, Landsat, and MODIS satellites, for example, provide high-resolution optical imagery that captures critical vegetation indices such as the Normalized Difference Vegetation Index (NDVI), Normalized Difference Water Index (NDWI), and Green Normalized Difference Vegetation Index (GNDVI). These indices are strongly correlated with crop health, biomass, and potential yield (Bendig *et al.,* 2015; Thenkabail*et al.,* 2018). However, optical sensors are affected by cloud cover, making

synthetic aperture radar (SAR) data invaluable for all-weather monitoring. Sentinel-1, a SAR satellite, provides backscatter information sensitive to surface roughness and moisture content, making it highly effective for agricultural area mapping and crop monitoring (Veloso *et al.,* 2017).

Crop simulation models, on the other hand, integrate biophysical processes governing crop growth and development to predict yield outcomes. Models such as the Decision Support System for Agrotechnology Transfer (DSSAT) and the Agricultural Production Systems sIMulator (APSIM) simulate yield based on inputs including weather conditions, soil properties, and crop management practices (Jones *et al.,* 2003; Keating *et al.,* 2003). Despite their strengths, these models often require precise, spatially explicit inputs that are challenging to obtain.

The integration of remote sensing data with crop simulation models addresses key limitations in both approaches. Remote sensing provides real-time, spatially explicit observations that can calibrate and validate simulation models, enhancing yield predictions at fine spatial resolutions. This combined approach enables the generation of spatially detailed yield maps, supporting precision agriculture and resource optimization (Lobell *et al.*, 2015).

In this research, we develop a framework for spatial yield estimation that integrates Sentinel-1 SAR data for area estimation with a crop simulation model for yield prediction. Our study focuses on Bengal gram (Cicer arietinum) cultivation in Nagaur district, Rajasthan, India - a region characterized by semi-arid climatic conditions and significant agricultural activity. Sentinel-1 backscatter data is used to map crop area, while the crop simulation model incorporates biophysical parameters to predict yield. By integrating these data, we generate spatially explicit yield maps that provide actionable insights for agricultural management and policy planning.

2. MATERIAL AND METHODS

2.1 Study Area

Nagaur district, located in the central part of Rajasthan state, India, covers an area of approximately 17,718 square kilometers. It lies between latitudes 26°25′N and 27°40′N and longitudes 73°37′E and 75°22′E (Fig. 1). The district is known for its predominantly semi-arid climate, characterized by hot summers and mild winters. The average annual rainfall ranges from 300 to 500 mm, with most precipitation occurring during the monsoon season from July to September. Temperatures in the region can vary significantly, reaching up to 45°C in summer and dropping to around 5°C in winter.

Agriculture is the primary livelihood in Nagaur district, with a significant portion of the population engaged in farming activities. The district's major crops include wheat, mustard, and pulses, with Bengal gram (Cicer arietinum) being one of the most important pulse crops. The region's soils are predominantly sandy, with varying levels of fertility. Due to the arid conditions, groundwater and canal irrigation are critical for sustaining agricultural productivity. The combination of challenging climatic conditions and reliance on irrigation makes the region suitable for applying advanced remote sensing and crop simulation technologies to enhance yield estimation and agricultural management.

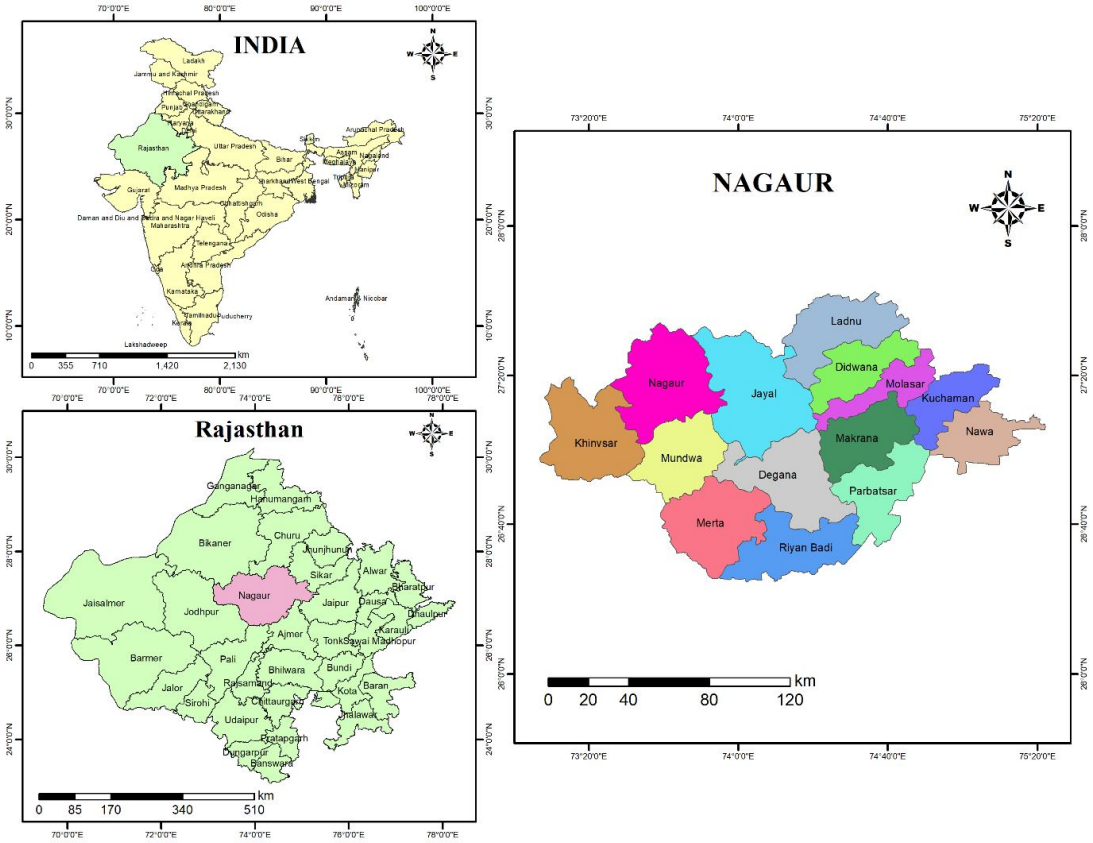

Fig. 1. Location of Study Area

2.2 Satellite Data

This study utilizes Sentinel-1A SAR satellite data from the European Space Agency (ESA) for crop area estimation in Nagaur district, Rajasthan, India. Sentinel-1A operates in the C-band microwave frequency range, enabling all-weather, day-and-night data acquisition. It offers dual polarization (VH and VV) and provide data 12-days interval. The satellite operates in four standard modes: Strip Map (SM), Extra Wide Swath (EW), Interferometric Wide Swath (IW), and Wave Mode (WV). For this research, Interferometric Wide Swath (IW) Ground Range Detected (GRD) products were used.

Sentinel-1A data from August 2022 to March 2023 was acquired at 12-day intervals from the Copernicus Open Access Hub. This time-series SAR data supports robust crop area mapping and yield estimation by integrating with the crop simulation model for the Rabi season. Table 1 provide details about Sentinel 1A satellite.

Table 1. Details of Sentinel-1A (IW-GRD) data

S.No	Parameters	Characteristics
1.	Pixel value	Magnitude detected
2.	Coordinate system	Ground range

3.	Polarization options	Single (VV or HH) or Dual (HH+HV or VV+VH)
4.	Look overlap (range, azimuth)	0.250, 0.000
5.	Resolution (range x azimuth in meters)	20.4 x 21.7
6.	Bits per pixel	16
7.	Pixel spacing (range x azimuth in meters)	10 x 10
8.	Radiometric resolution	1.7 dB
9.	Incidence angle (degree)	32.9
10.	Ground range coverage (km)	251.8
11.	Equivalent Number of Looks (ENL)	4.4
12.	Absolute location accuracy (m)	7
13.	Number of looks (range x azimuth)	5 x 1
14.	Azimuth look bandwidth (Hz)	327
15.	Range look bandwidth (Hz)	14.1
Source: (De Zan and Guarnieri, 2006)		

2.3 Bengal gram area mapping

2.3.1 SAR Data Preprocessing

The Sentinel-1A SAR data from the European Space Agency (ESA) were preprocessed using MAPscape software developed by sarmap (Switzerland). The software incorporated an automated processing chain based on the methodology proposed by Holecz *et al.* (2013). The main processing steps involved are:

- **Strip Mosaicking**: Individual SAR image frames from the same orbit and acquisition date were mosaicked to generate continuous strips, facilitating seamless data management and processing.
- **Co-registration**: Multi-temporal images were geometrically aligned using co-registration, which is a prerequisite for effective time-series analysis and speckle filtering (Raman *et al.,* 2019).
- **Time-Series Speckle Filtering**: A multi-temporal filter by De Grandi *et al.* (1997) was applied to reduce speckle noise while preserving the reflectivity of stable objects.
- **Terrain Geocoding and Radiometric Calibration**: Digital Elevation Model (DEM) data were used to convert the SAR data into geocoded σ° values in a cartographic reference system. Radiometric normalization was applied to correct for range and angle dependencies (Ramalingam *et al.,* 2019; Venkatesan *et al.,* 2019; Karthikkumar*et al.,* 2019)
- **ANLD Filtering and Atmospheric Correction**: Adaptive Non-Local Means filtering (ANLD) was employed to smooth homogeneous areas and enhance feature boundaries. Corrections for atmospheric attenuation due to water vapor and heavy

rainfall were applied using temporal signature anomaly detection techniques (Aspert *et al.,* 2007).

2.3.2 Parameterized Classification

Based on the temporal signature in the monitoring fields, parameters viz., (i) minima and (ii) maxima of those mean σ° values across monitoring fields; the (iii) maxima of the minimum σ° values; the (iv) minima of the maximum σ° values across fields; and the (v) minimum and (vi) maximum of the range of σ° values across fields will be generated. The value of the six temporal features from the monitoring locations will be used to guide the choice of the six parameter values (Table 2).

Table 2. Site-specific parameters for rule-based classification and the criteria employed to select them based on temporal features

Parameter	Relationship between Parameter and Temporal Feature
a = lowest mean	a < (i) minima of the mean σ° across all signatures
b = highest mean	b > (ii) maxima of the mean σ° across all signatures
c = maximum variation	c > (vi) maxima of the range in σ° across all signatures
d = max value at SoS	d > (iii) highest minima in σ° across all signatures
e = min value at the peak	e < (iv) lowest maxima in σ° across all signatures
f = minimum variation	f < (v) minima of the range in σ° across all rice signatures

The process of crop area estimation involving multi-temporal feature extraction and parameterized classification from MAPscape software is presented in Fig. 2.

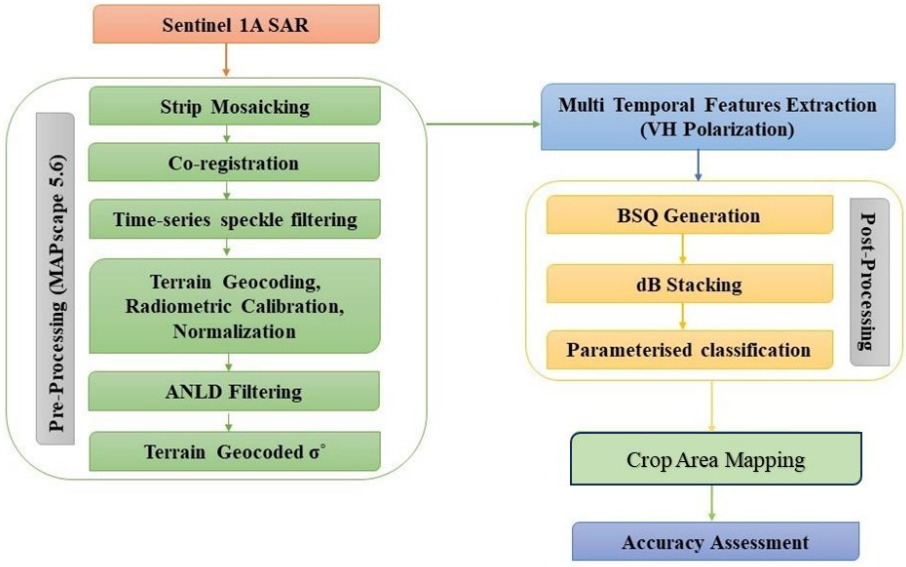

Fig. 2. Schematic representation of the processing of SAR data and estimation of crop area

2.3.3 Accuracy Assessment

The accuracy of the crop area map was evaluated using ground truth data. A standard confusion matrix was constructed, with validation points categorized as crop or non-crop. Accuracy metrics included:

- **Overall Accuracy:** The percentage of correctly classified points.
- **Kappa Coefficient**: A statistical measure of classification reliability accounting for chance agreement.

2.4 Yield Estimation

2.4.1 Crop Yield Simulation using the DSSAT Model

The Decision Support System for Agro-technology Transfer (DSSAT) was developed through international collaboration under IBSNAT, USA (Jones *et al.,* 2003). It integrates crop, soil, and weather data for evaluating crop management practices across different locations and years. In this study, the DSSAT model was used for yield simulation.

2.4.2 CROPGRO-Bengal gram

Crop growth and development were simulated daily using the CROPGRO-Bengal gram modules within DSSAT v4.8 (Fig. 3). The model calculates daily changes in soil water content by accounting for processes like infiltration, irrigation, drainage, evaporation, transpiration, and root water uptake. Cultivar coefficients served as key input parameters.

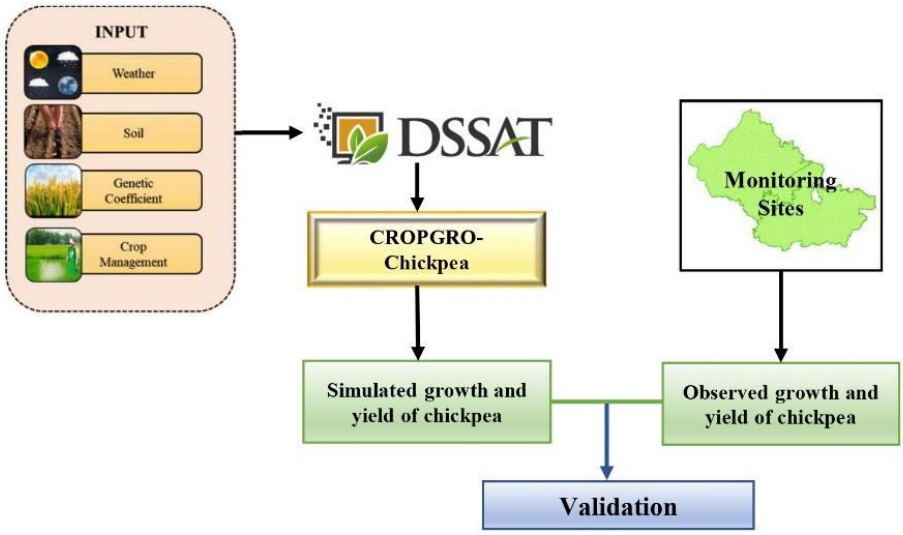

Fig. 3. Schematic representation of methodology of DSSAT CROPGRO-Bengal gram crop simulation model

a) **Weather Data:** Daily maximum and minimum temperatures, solar radiation, and rainfall were processed using the DSSAT Weather Man tool.
b) **Soil Data:** Soil profiles were sourced from the Harvard Dataverse for Nagaur district.
c) **Cultivar Data:** Genetic coefficients for Bengal gram varieties were specified.
d) **Crop Management:** Data on planting geometry, irrigation, fertilization, and tillage were input using the DSSAT X Build tool.

Model calibration was performed using observed field data, and validation was achieved by comparing simulated and observed yields.

2.4.3 LAI Estimation from SAR Data

Leaf Area Index (LAI) was estimated from backscatter (dB) values of Sentinel-1A SAR images. Using QGIS, backscatter values from field plots were sampled and regressed against DSSAT-simulated LAI. The resulting regression model enabled spatial LAI extraction.

2.4.4 Yield estimation using remote sensing techniques

The DSSAT simulated yield was integrated with the remote sensing data using LAI values extracted from dB images of the SAR data. A linear regression equation was created to calculate crop yield for the research area using the DSSAT simulated yield and spatially simulated LAI values (Fig. 4).

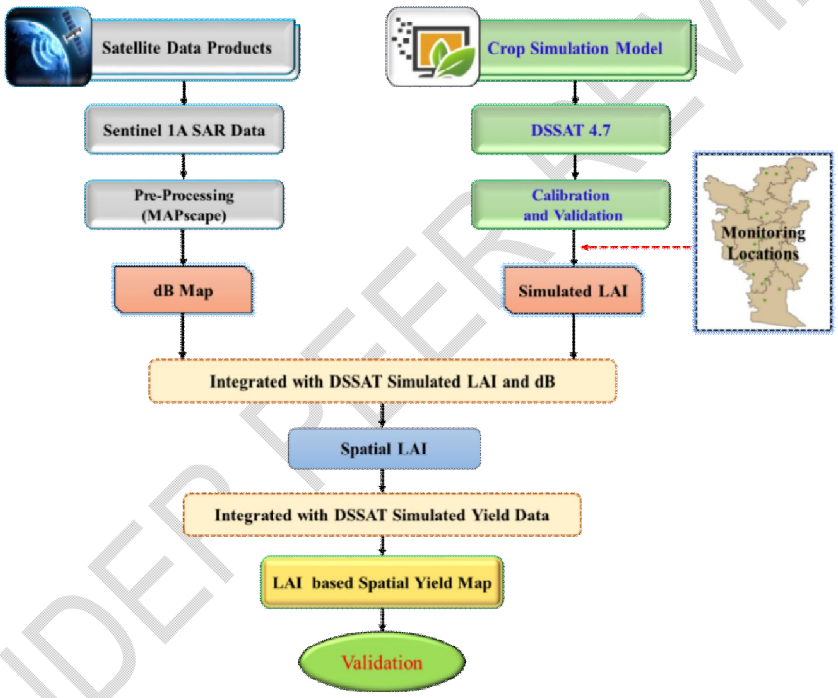

Fig. 4. Schematic representation of the crop yield estimation by integrating SAR satellite products and the DSSAT crop simulation model

2.4.5 Statistical evaluation and validation of products

Spatial yield estimated from remote sensing products integrated with DSSAT model were validated with actual yield observed in the farmer's field. In addition, the extracted yields were validated with CCE data.

An analysis of the degree of coincidence between estimated and observed values was carried out using R^2, Root Mean Square Error (RMSE), Normalized Root Mean Square Error (NRMSE) and agreement per cent.

$$NRMSE = 100 \times (RMSE / Oi)$$

$$Agreement\ (\%) = 100 \times (1 - (RMSE / Oi))$$

Pi and Oi are the predicted and observed values for the observation, and N is the number of observations within each treatment. RMSE is a measure of the deviation of the simulated from the measured values and is always positive. A zero value is ideal. The lower the value of RMSE, the higher the accuracy of the model prediction.

3. RESULTS AND DISCUSSION

3.1 Area mapping

The classified Bengal gram area in the Nagaurdistrict was assessed to be 1,41,336 ha. Among 13 blocks in Nagaur district, the highest Bengal gram area was recorded in Merta block followed by Kuchaman block with an area of 22,333 and 20,518 ha, respectively. Riyan Badi and Degana blocks recorded 16,116 and 14,508 ha of Bengal gram area, respectively. The Didwana block, it accounted for 11,664 ha of Bengal gram area (Table 3 &Fig. 5). The substantial variation in Bengal gram cultivation areas among different blocks can be attributed to several factors, including soil fertility, water availability, and agricultural practices (Pazhanivelan*et al,* 2022).

Table 3. Block-wise Bengal gram area for Nagaurdistrict during *Rabi* season 2022

S.No	Block Name	Area (ha)
1.	Degana	14508
2.	Didwana	11664
3.	Jayal	8953
4.	Kheenvsar	9852
5.	Kuchaman	20518
6.	Ladnu	5545
7.	Makrana	3373
8.	Merta	22333
9.	Mundwa	9888
10.	Nagaur	1944
11.	Nawa	9870
12.	Parbatsar	6773
13.	Riyan Badi	16116
Total Area		**141336**

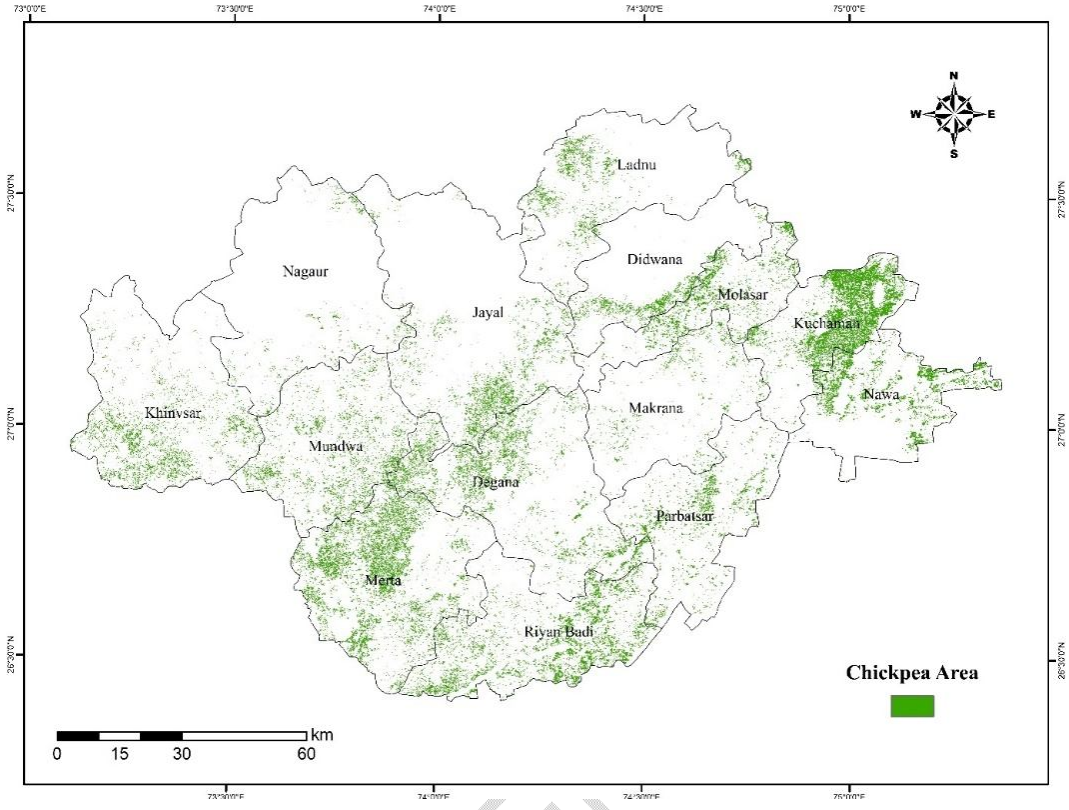

Fig. 5. Bengal gram area for Nagaur district

3.2 Assessment of accuracy

The assessment of accuracy for the Bengal gram area map was steered with the Bengal gram and non-Bengal gram class-based ground truth points. In the study area using the random stratified sampling method, 200 Bengal gram and 61 non-Bengal gram points were collected and considered for validation. The overall map accuracy for the Bengal gram area was 85.1 per cent with average reliability of 79.3 per cent. A measure of excellence of classification *i.e.,* The kappa index was identified to be 0.70 indicating the estimation with good accuracy in the Nagaur district during *Rabi* season 2022 (Table 4).

Table 4. Accuracy assessment of Bengal gram classification from SAR data

		Predicted class from the map		
Actual class from survey	**Class**	**Bengal gram**	**Non-Bengal gram**	**Accuracy (%)**
	Bengal gram	169	31	84.5
	Non-Bengal gram	8	53	86.9
	Reliability	95.5	63.1%	85.1
Average accuracy		85.7%		
Average reliability		79.3%		
Overall accuracy		85.1%	**Good Accuracy**	
Kappa index		0.70	**Good Accuracy**	

4.3.3 LAI of Bengal gram at spatial level

LAI values were spatially developed for the study area by integrating the dB values along with DSSAT-simulated LAI values in the monitoring locations of the study area (Fig. 6). These results align with previous studies showing the efficacy of remote sensing and the DSSAT model for accurate LAI predictions (Baret & Buis, 2008; Zhao *et al.,* 2010; Kang *et al.,* 2021; Hoogenboom *et al*., 2019). Both methods exhibited low RMSE and NRMSE values, indicating precise estimates close to observed values. The consistent high agreement percentages across different LAI ranges suggest that both RS and DSSAT models perform well under various conditions, enhancing their applicability in diverse agricultural settings. Accurate LAI predictions are crucial for effective crop management, as LAI is a key indicator of photosynthetic capacity and overall plant health (Cheng *et al.,* 2022).

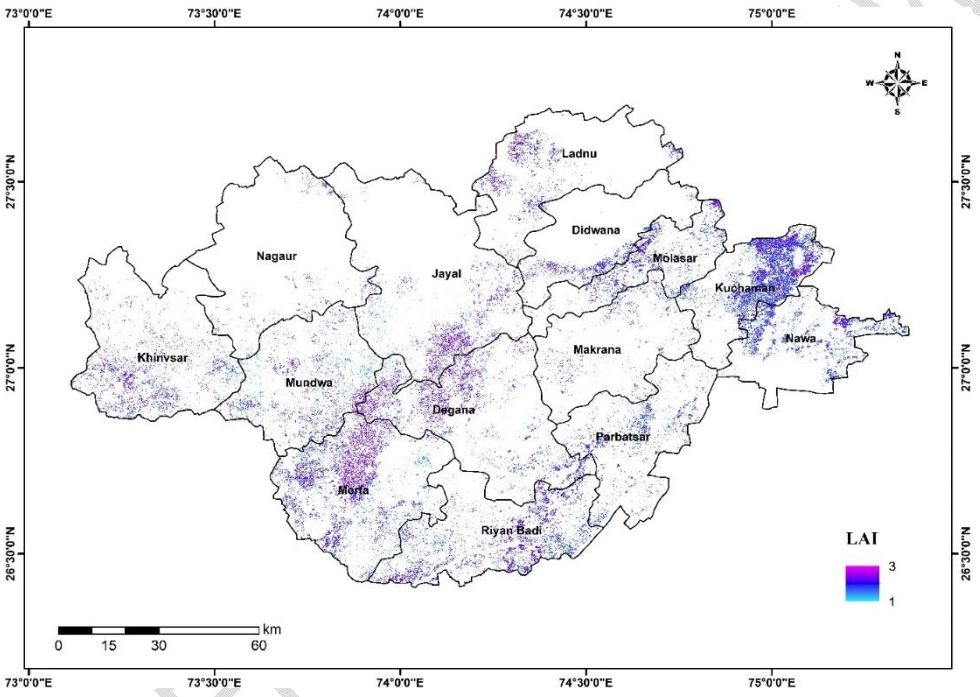

Fig. 6. Spatial LAI map of Nagaur district

3.4 Spatial Bengal gram yield estimation

Depending on the spatially developed LAI for the study area, the regression model was used to generate the Bengal gram yield spatially (Fig. 7). Estimates of Bengal gram end-of season yields produced by integrating remote sensing tools with the DSSAT-CERES model. The DSSAT Bengal gram yields in the Nagaur area ranged from 952 kg/hato 1983 kg/ha (Table 5). The mean agreement between observed yields in monitoring locations and DSSAT spatial yields derived from satellites was found 91.3 per cent. Overall, both DSSAT and integrated remote sensing methods are effective for crop yield prediction. While DSSAT is valuable for detailed agronomic modeling, integrating remote sensing tools with crop simulation models offers an efficient alternative for rapid and large-scale yield estimation (Akumaga*et al.,* 2023; Pazhanivelan*et al.,* 2022). These tools significantly advance precision agriculture by facilitating better crop monitoring and management strategies.

Table 5. Agreement between Observed & Remote sensing-based yield

ID	Lat	Long	DSSAT (kg/ha)	CCE (kg/ha)	RMSE (kg/ha)	NRMSE (%)	Agreement (%)
1	26.77	74.43	989	1089	100	9.2	90.8
2	26.74	74.41	1056	1234	178	14.4	85.6
3	26.63	74.20	1497	1539	42	2.7	97.3
4	26.75	74.18	1392	1482	90	6.1	93.9
5	26.79	74.23	1023	1027	4	0.4	99.6
6	26.74	74.41	1983	2064	81	3.9	96.1
7	26.77	74.43	1684	1534	150	9.8	90.2
8	26.80	74.24	1168	1098	70	6.4	93.6
9	26.77	74.43	1287	1251	36	2.9	97.1
10	26.77	74.43	1254	1146	108	9.4	90.6
11	26.75	74.43	1456	1389	67	4.8	95.2
12	26.78	74.43	1265	1183	82	6.9	93.1
13	26.66	74.31	1687	1458	229	15.7	84.3
14	26.65	74.28	1892	1632	260	15.9	84.1
15	26.60	74.17	1326	1462	136	9.3	90.7
16	26.62	74.16	1464	1657	193	11.6	88.4
17	26.62	74.16	1455	1695	240	14.2	85.8
18	26.63	74.16	1469	1536	67	4.4	95.6
19	26.64	74.00	1686	1521	165	10.8	89.2
20	26.64	74.00	1466	1687	221	13.1	86.9
21	26.77	74.47	1352	1591	239	15.0	85.0
22	26.77	74.45	1602	1634	32	2.0	98.0
23	26.77	74.51	1562	1653	91	5.5	94.5
24	26.82	74.65	1401	1526	125	8.2	91.8
25	26.84	74.72	1628	1827	199	10.9	89.1
26	26.87	74.76	1278	1462	184	12.6	87.4
27	26.91	74.77	1102	1294	192	14.8	85.2
28	26.99	74.77	1646	1548	98	6.3	93.7
29	26.83	74.66	952	1068	116	10.9	89.1
30	26.84	74.73	1326	1298	28	2.2	97.8
Agreement					127	8.7	91.3

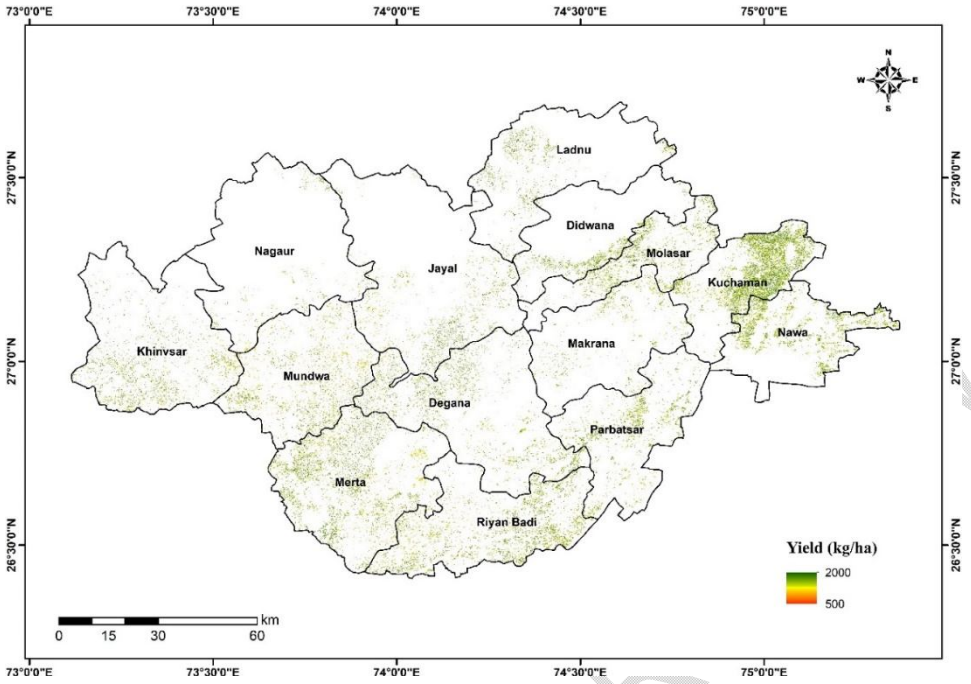

Fig. 7. Spatial yield map of Nagaur district during *Rabi* 2022

4. CONCLUSION

This research demonstrates the successful integration of Sentinel-1 SAR remote sensing data and the DSSAT crop simulation model for spatial yield estimation of Bengal gram in Nagaur district, India. The SAR-based classification achieved an overall accuracy of 85.1%, demonstrating the effectiveness of synthetic aperture radar for precise crop area mapping under challenging weather conditions. By linking remotely sensed leaf area index (LAI) with DSSAT-simulated yields, the framework produced spatially explicit yield maps with a high level of agreement (91.3%) between predicted and observed yields. This integrated approach offers several advantages, including reduced dependency on exhaustive field data collection, scalable yield prediction, and enhanced decision-making for agricultural planning.

The combined use of remote sensing and crop simulation models advances precision agriculture by enabling efficient monitoring of crop performance across large areas. This methodology can be adapted for other crops and regions, further supporting sustainable agricultural practices and food security. Future work can explore the integration of additional satellite sensors, advanced machine learning techniques, and refined parameterization of crop models to improve predictive accuracy and resilience against climate variability. The research underlines the transformative potential of geospatial technologies in modern agricultural systems, contributing to the optimization of resource use and improved agricultural productivity.

ABBREVIATIONS

CCE	:	Crop Cutting Experiment
dB	:	Decibels
DSSAT	:	Decision Support System for Agro-technology Transfer
GIS	:	Geographic Information System
ha.	:	Hectare
VIZ.,	:	Namely
%	:	Percentage
LAI	:	Leaf Area Indec
NRMSE	:	Normalized Root Mean Square Error
RMSE	:	Root Mean Square Error
SAR	:	Synthetic Aperture Radar
S1	:	Sentinel 1
S2	:	Sentinel 2
VH	:	Vertically Transmitted, Horizontally Received
VV	:	Vertically Transmitted, Vertically Received

REFERENCES

Akumaga, U., Gao, F., Anderson, M., Dulaney, W. P., Houborg, R., Russ, A., & Hively, W. D. (2023). Integration of remote sensing and field observations in evaluating DSSAT model for estimating maize and soybean growth and yield in Maryland, USA. Agronomy, 13(6), 1540. https://doi.org/10.3390/agronomy13061540

Aspert, F., Bach-Cuadra, M., Cantone, A., Holecz, F., &Thiran, J.-P. (2007). Time-varying segmentation for mapping of land cover changes. In Proceedings of ENVISAT Symposium, 23–27.

Baret, F., & Buis, S. (2008). Estimating canopy characteristics from remote sensing observations: Review of methods and associated problems. In Advances in Land Remote Sensing (pp. 173–201). Springer. https://doi.org/10.1007/978-1-4020-6450-0_7

Bendig, J., Bolten, A., &Bareth, G. (2015). Introducing a low-cost UAV for thermal- and multispectral-imaging. Remote Sensing, 7(3), 3074–3090. https://doi.org/10.3390/rs70303074

Cheng, E., Zhang, B., Peng, D., Zhong, L., Yu, L., Liu, Y., & Yang, S. (2022). Wheat yield estimation using remote sensing data based on machine learning approaches. Frontiers in Plant Science, 13, 1090970. https://doi.org/10.3389/fpls.2022.1090970

De Grandi, G. F., Leysen, M., Lee, J. S., & Schuler, D. (1997). Radar reflectivity estimation using multiple SAR scenes of the same target: Technique and applications. In IGARSS'97. 1997 IEEE International Geoscience and Remote Sensing Symposium Proceedings. Remote Sensing-A Scientific Vision for Sustainable Development (Vol. 2, pp. 1047-1050). IEEE.

De Zan, F., & Guarnieri, A. M. (2006). TOPSAR: Terrain observation by progressive scans. *IEEE Transactions on Geoscience and Remote Sensing*, *44*(9), 2352-2360.

Holecz, F., Barbieri, M., Collivignarelli, F., Gatti, L., Nelson, A., Setiyono, T. D., &Pazhanivelan, S. (2013). An operational remote sensing based service for rice production estimation at national scale. In Proceedings of the Living Planet Symposium. https://doi.org/10.13140/2.1.1492.8643

Hoogenboom, G., Porter, C. H., Boote, K. J., Shelia, V., Wilkens, P. W., Singh, U., & Hunt, L. A. (2019). The DSSAT crop modeling ecosystem. In Advances in Crop Modeling for a Sustainable Agriculture (pp. 173–216). Elsevier.

Jones, J. W., Hoogenboom, G., Porter, C. H., Boote, K. J., Batchelor, W. D., Hunt, L. A., ... & Ritchie, J. T. (2003). The DSSAT cropping system model. European journal of agronomy, 18(3-4), 235-265. https://doi.org/10.1016/S1161-0301(02)00107-7

Kang, Y., Ozdogan, M., Gao, F., Anderson, M. C., White, W. A., Yang, Y., & Erickson, T. A. (2021). A data-driven approach to estimate leaf area index for Landsat images over the contiguous US. Remote Sensing of Environment, 258, 112383. https://doi.org/10.1016/j.rse.2021.112383

Karthikkumar, A., Pazhanivelan, S., Jagadeeswaran, R., Ragunath, K., &Kumaraperumal, R. (2019). Generating banana area map using VV and VH polarized radar satellite image. Madras Agricultural Journal, 106(1-6).

Keating, B. A., Carberry, P. S., Hammer, G. L., Probert, M. E., Robertson, M. J., Holzworth, D., ... & Smith, C. J. (2003). An overview of APSIM, a model designed for farming systems simulation. European journal of agronomy, 18(3-4), 267-288. https://doi.org/10.1016/S1161-0301(02)00108-9

Lobell, D. B., Thau, D., Seifert, C., et al. (2015). A scalable satellite-based crop yield mapper. Remote Sensing of Environment, 164, 324–333. https://doi.org/10.1016/j.rse.2015.04.021

Pazhanivelan, S., Geethalakshmi, V., Tamilmounika, R., Sudarmanian, N. S., Kaliaperumal, R., Ramalingam, K., & Quicho, E. D. (2022). Spatial rice yield estimation using multiple linear regression analysis, semi-physical approach, and assimilating SAR satellite derived products with DSSAT crop simulation model. Agronomy, 12(9), 2008. https://doi.org/10.3390/agronomy12092008

Ramalingam, K., Ramathilagam, A. B., & Murugesan, P. (2019). Area estimation of cotton and maize crops in Perambalur district of Tamil Nadu using multi-date Sentinel-1A SAR data & optical data. The International Archives of the Photogrammetry, Remote Sensing and Spatial Information Sciences, 42, 137–140.

Raman, M. G., Kaliaperumal, R., Pazhanivelan, S., & Kannan, B. (2019). Rice area estimation using parameterized classification of Sentinel-1A SAR data. The International Archives of the Photogrammetry, Remote Sensing and Spatial Information Sciences, 42, 141–147.

Thenkabail, P. S., Lyon, J. G., & Huete, A. (Eds.). (2018). Hyperspectral remote sensing of vegetation. CRC Press.

Veloso, A., Mermoz, S., Bouvet, A., Le Toan, T., Planells, M., Dejoux, J. F., &Ceschia, E. (2017). Understanding the temporal behavior of crops using Sentinel-1 and Sentinel-2-like data for agricultural applications. Remote sensing of environment, 199, 415-426. https://doi.org/10.1016/j.rse.2017.07.015

Venkatesan, M., Pazhanivelan, S., &Sudarmanian, N. (2019). Multi-temporal feature extraction for precise maize area mapping using time-series Sentinel-1A SAR data. The International Archives of the Photogrammetry, Remote Sensing and Spatial Information Sciences, 42, 169–173.

Zhao, D., Reddy, K. R., Kakani, V. G., Read, J. J., & Koti, S. (2010). Canopy reflectance in cotton for growth assessment and lint yield prediction. European Journal of Agronomy, 32(1), 35–42. https://doi.org/10.1016/j.eja.2006.12.001